Atmos. Chem. Phys. Discuss., 15, 33555–33582, 2015
www.atmos-chem-phys-discuss.net/15/33555/2015/
doi:10.5194/acpd-15-33555-2015

Atmospheric Chemistry and Physics Discussions
Open Access

Quantification of black carbon mixing state from traffic: implications for aerosol optical properties

M. D. Willis[1], R. M. Healy[2,3,a], N. Riemer[4], M. West[5], J. M. Wang[2], C.-H. Jeong[2], J. C. Wenger[3], G. J. Evans[2], J. P. D. Abbatt[1], and A. K. Y. Lee[1]

[1]Department of Chemistry, University of Toronto, Ontario, Canada
[2]Southern Ontario Centre for Atmospheric Aerosol Research, Department of Chemical Engineering and Applied Chemistry, University of Toronto, Ontario, Canada
[3]Department of Chemistry and Environmental Research Institute, University College Cork, Cork, Ireland
[4]Department of Atmospheric Sciences, University of Illinois at Urbana-Champaign, Urbana, USA
[5]Department of Mechanical Science and Engineering, University of Illinois at Urbana-Champaign,Urbana, USA
[a]now at: Air Monitoring and Transboundary Air Sciences Section, Environmental Monitoring and Reporting Branch, Ontario Ministry of the Environment and Climate Change, Ontario, Canada

Received: 11 November 2015 – Accepted: 16 November 2015 – Published: 27 November 2015

Correspondence to: M. D. Willis (megan.willis@mail.utoronto.ca) and A. K. Y. Lee (alexky.lee@utoronto.ca)

Published by Copernicus Publications on behalf of the European Geosciences Union.

Abstract

The climatic impacts of black carbon (BC) aerosol, an important absorber of solar radiation in the atmosphere, remain poorly constrained and are intimately related to its particle-scale physical and chemical properties. Using particle-resolved modelling informed by quantitative measurements from a soot-particle aerosol mass spectrometer, we confirm that the mixing state (the distribution of co-emitted aerosol amongst fresh BC-containing particles) at the time of emission significantly affects BC-aerosol optical properties even after a day of atmospheric processing. Both single particle and ensemble aerosol mass spectrometry observations indicate that BC near the point of emission co-exists with hydrocarbon-like organic aerosol in two distinct particle types: HOA-rich and BC-rich particles. The average mass fraction of black carbon in HOA-rich and BC-rich particles was 0.02–0.08 and 0.72–0.93, respectively. Notably, approximately 90 % of BC mass resides in BC-rich particles. This new measurement capability provides quantitative insight into the physical and chemical nature of BC-containing particles and is used to drive a particle-resolved aerosol box model. Significant differences in calculated single scattering albedo (an increase of 0.1) arise from accurate treatment of initial particle mixing state as compared to the assumption of uniform aerosol composition at the point of BC injection into the atmosphere.

1 Introduction

Incomplete combustion emits teragram quantities of black carbon (BC) aerosol to the troposphere each year, resulting in a significant warming effect on climate that may be second only to carbon dioxide (Bond et al., 2013; Ramanathan and Carmichael, 2008; Jacobson, 2001). BC influences climate directly, by absorbing solar radiation, and indirectly, by changing cloud properties and altering snow and ice melt. BC impacts on the global scale remain poorly constrained and are intimately related to its particle-scale physical and chemical properties (Bond et al., 2013). The majority of BC

ACPD
15, 33555–33582, 2015

emissions in North America, Europe and Latin America are derived from traffic-related sources, though the specific physical and chemical properties of BC-containing particles at emission depend greatly on the source (Bond et al., 2013). BC-containing particles are generally hydrophobic near emission and become mixed over time with hydrophilic species through condensation and coagulation (Johnson et al., 2005; Moteki et al., 2007; Moffet and Prather, 2009), with resulting impacts on particle hygroscopicity (McMeeking et al., 2011b; D. Liu et al., 2013; Laborde et al., 2013) and optical properties (Zhang et al., 2008; Cappa et al., 2012; Lack et al., 2012; Knox et al., 2009; Liu et al., 2015). Despite extensive previous work, our understanding of the role of mixing state in influencing the climate impacts of BC remains incomplete, in part because of instrumental challenges in particle characterization.

Studies assessing both the composition and amount of non-BC species in BC-containing particles are rare. A large body of evidence from urban, tunnel and engine emission studies has shown that individual combustion particles are mixtures of BC, inorganic species, metals, and hydrocarbon-like organic species at the time of emission (e.g., Johnson et al., 2005; Toner et al., 2006; Schneider et al., 2006; Tritscher et al., 2011; Chirico et al., 2010; Dallmann et al., 2014; Zhang et al., 2013; Massoli et al., 2012). Among these studies, single particle mass spectrometry has directly demonstrated mixing of BC and non-BC species in traffic-derived particles. For example, Toner et al. (2006) observed that emissions from heavy duty diesel engines were dominated by particles containing BC, organic species, calcium and phosphate, with one particle type dominated by BC and another with higher levels of organic species. In contrast, Healy et al. 2012 observed BC-dominated particles from traffic emissions in a European city. Other approaches to measure BC mixing state, including hygroscopicity and volatility differential mobility techniques, have highlighted the presence of an external mixture in terms of particle volatility with lower volatility, BC-containing aerosol being less hygroscopic (Kuwata et al., 2009; McMeeking et al., 2011a). Further, single particle soot photometer measurements of coating thickness in urban areas have shown that traffic-related BC-containing particles are largely uncoated or very thinly coated

(McMeeking et al., 2011b; Laborde et al., 2013; Shiraiwa et al., 2008; Liu et al., 2014). In addition, microscopy studies have illustrated the dominance of bare or thinly coated BC-containing particles in traffic emissions (China et al., 2014) and the occurrence of coating, embedding and compaction of BC as it is aged (Adachi et al., 2014; Adachi and Buseck, 2013). While previous work has provided valuable insight into BC mixing state, the majority of past approaches have not allowed simultaneous quantification of BC mixing state on a mass basis and chemical characterization of non-BC species.

Considerable attention has been paid to BC-containing aerosol because of the potential for short-term climate mitigation through emissions reduction (Shindell et al., 2012). Therefore, a quantitative understanding of BC mixing state is crucial for three reasons: first, to assess rates of BC processing and removal in the atmosphere; second, to assess the role that BC-containing particles play as cloud nuclei; and third, to assess direct effects on solar radiation. Aerosol optical properties are central parameters required to evaluate direct radiative forcing (DRF). One of the largest contributors to uncertainty in DRF calculations is the single scattering albedo (SSA) (McComiskey et al., 2008), defined as the ratio of aerosol scattering to total light extinction. Previous work has clearly demonstrated that calculations of aerosol optical properties depend upon assumptions about particle mixing state (e.g., Jacobson, 2000), with assumptions of uniform internal mixing producing overestimations in absorption efficiency and single scattering albedo (Zaveri et al., 2010; Matsui et al., 2013; Oshima et al., 2009). The role of BC-aerosol mixing state at emission in affecting its mixing state in the atmosphere has also been highlighted in modelling studies explicitly treating detailed aerosol micro-physical and chemical processes (e.g., Matsui et al., 2013). However, model assessments driven by quantitative measurements of aerosol mixing state remain rare.

In this work, we use a soot-particle aerosol mass spectrometer, equipped with a light-scattering module, to determine the mixing state of BC-containing particles from traffic-dominated sources in an urban environment. These measurements provide quantitative insight into the physical and chemical nature of BC-containing particles near emission, and are used to drive a particle-resolved aerosol box model to assess the effect of accurately representing BC mixing on aerosol optical properties.

2 Methods

2.1 SP-AMS measurements

A soot-particle aerosol mass spectrometer (SP-AMS, Aerodyne Research Inc., Billerica, MA, USA), equipped with a light scattering module, was deployed in two urban studies to assess the mixing state of rBC-containing particles derived from vehicle emissions (Lee et al., 2015). The first study was conducted in downtown Toronto away from major roadways ("non-roadside"), and the second was performed at ground level, near a busy road in downtown Toronto ("roadside"), to investigate fresh vehicle emissions. The SP-AMS was operated such that both rBC-containing particles and non-rBC-containing particles were detected in the non-roadside study (see Sect. S2 in the Supplement), whereas exclusively rBC-containing particles were detected in the roadside study (Lee et al., 2015; Onasch et al., 2012). The non-roadside site is described in detail in Lee et al. 2015. The roadside study took place from 31 May to 24 June 2013 at the Southern Ontario Centre for Atmospheric Aerosol Research (SOCAAR) facility in downtown Toronto, Canada, located at ground level and adjacent to a road with traffic volumes ranging from 16 000 to 25 000 vehicles day^{-1} (Sabaliauskas et al., 2014). Ambient air was sampled at 170 L min^{-1} through a 10 cm (inner diameter) stainless steel tube fitted with a 2.5 µm cut-off inlet, located 15 m from the roadside at a height of 3 m a.g.l.

Details of the SP-AMS (and SP-AMS with light scattering) have been described elsewhere (Lee et al., 2015; Onasch et al., 2012). The SP-AMS detects black carbon, which evaporates at ∼ 4000 K, as C_x^+ fragments (predominantly m/z 12, 24, 36, 48 and 60) and is referred to as refractory black carbon (rBC) (Onasch et al., 2012). We use the term "black carbon" (BC) when referring generally to the concept of "soot"-type aerosol, while rBC is used when referring to quantities measured by the SP-AMS. In the SP-AMS, rBC and associated species are volatilized in an infrared laser beam (1064 nm) and are ionized using 70 eV electron impact ionization followed by detection in a time-of-flight mass spectrometer (ToF-MS) operated in “V-mode.” For the majority of the study the SP-AMS was operated at one-minute time resolution alternating between bulk mass spectrum (MS), particle time-of-flight (pToF) and single particle modes. The SP-AMS was operated at high-time resolution (1 Hz) in MS mode for a total of five days during the roadside study. SP-AMS data was analysed using the Igor Pro-based analysis tool PIKA (Seuper, 2010). The single particle categorization procedure and *k*-means clustering algorithm used to analyse the single particle data followed the description in Lee et al. (2015). Positive matrix factorization (PMF) analysis of ensemble data was performed to identify the sources of rBC and organics based on procedures described previously (Paatero and Tapper, 1994; Zhang et al., 2011; Ulbrich et al., 2009).

Without the tungsten vaporizer, direct calibrations of the ionization efficiency for NH_4NO_3 (IE_{NO_3}) are not possible. Therefore, size-selected (300 nm) Regal Black (Regal 400R Pigment, Cabot Corp.) particles were used to determine the mass based ionization efficiency of rBC (mIE_{rBC}) (Onasch et al., 2012; Willis et al., 2014). The relative ionization efficiency for rBC ($RIE_{rBC} = mIE_{rBC}/mIE_{NO_3}$) was 0.2 ± 0.05, as experimentally determined before removal of the tungsten vaporizer. Assuming that RIE_{rBC} is constant, IE_{NO_3} could be calculated based on known values of mIE_{rBC} and RIE_{rBC}. The average mIE_{rBC} was 189 ± 20 ions pg^{-1} in the roadside study. The calculated IE_{NO_3} was then used with recommended relative ionization efficiencies to quantify other aerosol species associated with rBC (Jimenez et al., 2003). Collection efficiency for rBC particles was determined in the roadside study using beam width probe (BWP) measurements described in (Willis et al., 2014). Ambient rBC-containing particles had an average beam width $\sigma = 0.46 \pm 0.03$ mm, which is close to, but wider than that of 300 nm Regal Black particles ($\sigma = 0.40 \pm 0.08$ nm) (Willis et al., 2014). Therefore, a collection efficiency (CE) of 0.6 was applied for absolute quantification of rBC and associated species. A time-varying collection efficiency was not possible with BWP measurements available here; the assumption of a constant CE over periods of local and long-range transport influence in this study provided a good linear correlation with PASS absorption measurements (405 and 781 nm) and SP-AMS rBC (Healy et al., 2015, Fig. 4). Note that the CE applied will not impact calculations of mf_{rBC}; however, there are uncertainties in the recommended RIE for organic species for the SP-AMS of up to $\sim 50\,\%$ (Lee et al., 2015; Willis et al., 2014) that can impact these calculations. SP-AMS CE and quantification are discussed in further detail in Sect. S1 in the Supplement.

2.2 Particle-resolved box model

We used the stochastic particle-resolved box model PartMC-MOSAIC (Particle Monte Carlo – Model for Simulating Aerosol Interactions and Chemistry) (Riemer et al., 2009; Zaveri et al., 2008) to quantify the importance of the observed mixing state information for the calculation of CCN and aerosol optical properties. PartMC-MOSAIC is suited for this task, as it explicitly tracks the composition of individual aerosol particles (in our case about 10^5 particles) in a population of different particle types within a well-mixed computational volume. Particle emissions, dilution with the background, and Brownian coagulation are simulated stochastically with PartMC, by generating a realization of a Poisson process using weighted particles in the sense of DeVille et al. (DeVille et al., 2011) and an accelerated binned sampling strategy (Michelotti et al., 2013). Coupled to PartMC is the MOSAIC chemistry code, which simulates gas chemistry (Zaveri and Peters, 1999), particle phase thermodynamics (Zaveri et al., 2005a, b), and dynamic gas-particle mass transfer (Zaveri et al., 2008) in a deterministic manner. An important update to previous work is the sampling algorithm to assign the composition of individual particles of initial condition and particle emissions. We now allow for stochastic composition variation at each diameter, with a prescribed standard deviation around a mean value. These parameters are quantitatively derived from measurements as described in Sect. S6 in the Supplement.

ACPD
15, 33555–33582, 2015

The set-up of the simulations was similar to the urban plume scenarios presented in Riemer et al. (2009) and Zaveri et al. (2010). We tracked the evolution of gas phase species and aerosol particles in a Lagrangian air parcel that was advected over and beyond a large urban area. The simulation started at 06:00 local standard time (LST) and, during the advection process, primary trace gases and aerosol particles from traffic sources were emitted into the air parcel for 12 h. After 18:00 LST, the emissions stopped, and the evolution of the aerosol population was tracked for another 12 h. More details can be found in Sect. S7 in the Supplement.

From the information on per-particle composition it is straightforward to calculate per-particle properties, such as hygroscopicity (Riemer et al., 2010; Zaveri et al., 2010; Ching et al., 2012; Tian et al., 2014; Fierce et al., 2013), optical properties (Zaveri et al., 2010), and particle reactivity (Kaiser et al., 2011), and to reconstruct the properties of the entire population.

3 Results and discussion

3.1 Two classes of fresh black carbon particles

Based on single particle SP-AMS measurements and using a particle categorization procedure and clustering algorithm described in our previous work (Lee et al., 2015), two types of particles originating from vehicle exhaust are identified in both roadside and non-roadside studies (Figs. 1 and S1 in the Supplement); HOA-rich and rBC-rich particle classes. The mass spectra of HOA-rich particles (Fig. 1a) exhibit fragmentation patterns associated with hydrocarbon structures (e.g., m/z 43 ($C_3H_7^+$), 57 ($C_4H_9^+$), 71 ($C_5H_{11}^+$)), and are consistent with previous aerosol mass spectrometer observations of gasoline/diesel vehicle exhaust and unburned lubricating oil (Massoli et al., 2012; Canagaratna et al., 2004; Mohr et al., 2009). The average mass fractions of rBC (mf_{rBC}) in HOA-rich particles during the non-roadside and roadside studies are very low: 0.03 and 0.05, respectively. The narrow distribution of mf_{rBC} (Figs. 2a and S1b in the Supplement) suggests that most of the HOA-rich particles are either mixed with a small amount of rBC or do not contain detectable rBC mass.

Mass spectra of rBC-rich particles are dominated by C_x^+ fragments (i.e., m/z 12, 24, 36, 48 and 60 in Fig. 1d) arising from black carbon. Smaller signals associated with HOA-like material in these particles are similar to the primary organic materials derived from diesel engine exhaust observed in laboratory studies (Sage et al., 2008). In contrast to the HOA-rich particles, Figs. 2c and S1d in the Supplement illustrate a range of mf_{rBC} values in rBC-rich particles. In the non-roadside and roadside environments the average mf_{rBC} values (±1 standard deviation) in this particle class are 0.72 (±0.18) and 0.86 (±0.14), respectively, highlighting the possibility that condensation and/or coagulation of HOA material on rBC particles might occur within a short time of emission. Assuming a "core-shell" structure, these observations demonstrate that rBC-rich particles are only very thinly coated with HOA-material, as compared to HOA-rich particles that have only very small rBC inclusions (Sect. S3, Fig. S2 in the Supplement).

3.2 Black carbon mass is dominated by black carbon rich particles

Single particle measurements provide direct insight into mixing state at an individual particle level; however, single particle detection has an inherent bias towards large particle sizes because light scattering triggers particle detection (Lee et al., 2015; Cross et al., 2009; Freutel et al., 2013; S. Liu et al., 2013). Ensemble size distributions of rBC peaked at ~100 nm in both roadside and non-roadside studies indicating that fresh rBC-containing particles emitted from vehicle exhaust are small (Figs. 3a and S3a in the Supplement). Smaller rBC-containing particles fall below the lower size limit of single particle detection (Fig. 3b and S3b in the Supplement). Therefore, single particle observations do not necessarily quantify mixing state at the population level. To provide a complementary view of rBC mixing state we turn to ensemble measurements. Ensemble measurements better represent mixing state on a population basis compared to single particle observations, because they cover a wider range of particle size (i.e., 80–1000 nm vacuum aerodynamic diameter, d_{va}).

By measuring very close to a busy road, ensemble SP-AMS observations of rBC and organic aerosol enabled the analysis of more than one hundred vehicle exhaust plumes over the course of the roadside study (Fig. 4a and b). Positive matrix factorization (PMF) (Zhang et al., 2011; Ulbrich et al., 2009) indicates three major sources of rBC and organic aerosol in the roadside environment: transported biomass burning (BBOA), regional background (OOA), and traffic emissions comprised of two PMF factors (HOA-rich and rBC-rich factors, Fig. 4c–f). Mass spectra of all four PMF factors and a discussion of selection of the number of factors is presented in Sect. S5 in the Supplement. Not previously observed with an AMS, the HOA- and rBC-rich factors represent two types of vehicle exhaust plumes with different amounts of rBC and HOA (Fig. 1b and e). The mf_{rBC} of HOA- and rBC-rich factors are 0.16 and 0.75, respectively. High-time resolution SP-AMS measurements (Fig. 5) also demonstrated varying organic and rBC levels in vehicle plumes (Fig. 1e and f), with corresponding differences in optical properties (SSA at 405 nm) indicating that rBC-rich plumes were more highly absorbing. The origin of different plume types at this site has been characterized through long-term measurements, and is related to a variety of engine types, operating conditions and pollution control features (Wang et al., 2015).

Figure 1b and e show the mass spectra of HOA- and rBC-rich PMF factors, which are strikingly similar to the mass spectra of HOA- and rBC-rich particle classes identified in the single particle measurements (Fig. 1a and d), validating the division of traffic emissions into the two factors observed here. The single particle and ensemble mass spectra show some differences. First, the HOA-rich factor has a larger rBC content compared to the HOA-rich particle class; second, the rBC-rich factor contains higher CO^+ and CO_2^+ signals compared to the rBC-rich particle class (inserts of Fig. 1d–f). The latter difference arises because highly oxygenated organic fragments (m/z 28 (CO^+) and 44 (CO_2^+)) were excluded in the single particle analysis due to interference of air signals in UMR spectra (Lee et al., 2015). The former difference likely arises because of SP-AMS sensitivity to rBC and the probability of rBC detection in a single particle (Lee et al., 2015).

With support of direct measurements of single particle mixing state, this work presents the first interpretation of ensemble AMS results in terms of rBC and HOA mixing state. Using the intensity of the two traffic-related factors in plumes (Fig. 4d and f), we estimate that rBC-rich particles account for ~ 90 % of the observed total traffic-related rBC mass (Fig. 2d). In a similar manner, we estimate that ~ 60 % of the total HOA mass is due to HOA-rich particles (Fig. 2b). Purple dashed lines shown in Fig. 2b and d represent the inclusion of all CO_x^+ fragments (due to surface functionality of ambient rBC Corbin et al., 2014) in the calculation of rBC mass (see Supplement Sect. S1), providing similar results. Red dashed lines in Fig. 2a–c represent the effect of a 50 % overestimation of HOA mass (see Supplement Sect. S1), again providing similar results.

3.3 Black carbon mixing state at emission impacts modelled optical properties

These novel single particle and ensemble observations of rBC mixing state were used to initialize the particle-resolved aerosol box model PartMC-MOSAIC (Supplement Sect. S6 and S7) (Zaveri et al., 2008; Riemer et al., 2009), which simulates the evolution of aerosol due to condensation and coagulation in an idealized urban setting. We simulate two cases to isolate the impact of mixing state of rBC emissions on aerosol properties. First, a uniform mixing state case in which all particles are assigned identical composition at emission (measured average mf_{rBC}), and second, a measurement-constrained mixing state case where mf_{rBC} is prescribed directly from our mixing state observations. The evolution of dry mf_{rBC} over a 24 h period is illustrated in Fig. 6a and b for the two cases. As ageing proceeds mf_{rBC} shifts to lower values, but in the uniform initial composition case no particles ever have mf_{rBC} larger than ~ 45 %. Note that the bulk aerosol composition and number size distributions are identical in the two cases (Fig. S10 in the Supplement), and any differences in optical properties arise only due to the distribution of aerosol components amongst the particles.

Optical properties are determined for each particle in the population using Mie calculations and assuming a core-shell structure. We acknowledge that the underlying

ACPD
15, 33555–33582, 2015

assumptions of Mie calculations may not be appropriate for rBC-containing aerosol in the real atmosphere (e.g., Adachi et al., 2011; Scarnato et al., 2013), which is often not spherical and may not exhibit a core-shell configuration (e.g., China et al., 2015). In particular, the enhancement of rBC absorption due to non-absorbing coatings may be overestimated (Cappa et al., 2012; Healy et al., 2015), except in situations where rBC sources and ageing promote extensive coating (Liu et al., 2015; China et al., 2015). However, Mie calculations are commonly applied in regional and global models (Chung and Seinfeld, 2005; Zhao et al., 2013; Fast et al., 2006) to estimate optical properties, and we therefore include this comparison to illustrate the sensitivity to mixing state.

Consistent with previous studies (e.g., Zaveri et al., 2010; Matsui et al., 2013), we observe a difference in volume absorption and scattering coefficients (B_{abs} and B_{scat}, Fig. 6c), and a resulting increase of 0.1 in SSA from the uniform mixing state to the measurement-constrained case that is present during the emission period in the simulation and, notably, persists throughout ageing (Fig. 6d). No significant differences in calculated cloud condensation nuclei activity were observed in these simulations (Fig. S11 in the Supplement), owing to the very similar hygroscopicity of rBC and HOA species. Calculations of aerosol DRF are very sensitive to changes in SSA (McComiskey et al., 2008) (e.g., uncertainties in SSA on the order of only 0.02 can result in a DRF uncertainty of 1 $W m^{-2}$ for a particular particle type Chin et al., 2009), illustrating the importance of accurately measuring and simulating mixing state for calculating climatologically relevant aerosol properties.

4 Conclusions

We present mass-based measurements of the mixing state of black carbon-containing aerosol, using a soot-particle aerosol mass spectrometer, from traffic emissions in an urban environment. Observations from single particle mass spectrometry indicate that rBC co-exists with hydrocarbon-like organic aerosol (HOA) in two distinct particle types; those containing a larger mass fraction of rBC, and those containing a larger mass

ACPD
15, 33555–33582, 2015

fraction of HOA. Source apportionment of ensemble mass spectral observations using positive matrix factorization also indicates two types of rBC-containing aerosol related to traffic: rBC-rich and HOA-rich aerosol, validated by single particle observations. Ensemble measurements expand the particle size range over which mixing state can be investigated, providing a better insight into the mixing state of the particle population and indicating that approximately 90 % of rBC mass resides in rBC-rich particles. These measurements were used to drive the particle-resolved aerosol box model, PartMC-MOSAIC. Our results indicate an increase in SSA of ~ 0.1 when mixing state at the point of emission is treated accurately in the model, compared to the assumption of uniform mixing state. The approach described here for quantitative assessment of black carbon mixing state from traffic can also be used to assess mixing state from other sources, and to explore the evolution of mixing state during atmospheric processing. Such measurements will be crucial to drive accurate model assessment of black carbon climate impacts on a broader scale.

The Supplement related to this article is available online at doi:10.5194/acpd-15-33555-2015-supplement.

Acknowledgements. This work was financially supported by Natural Sciences and Engineering Research Council (NSERC) of Canada, Environment Canada, the Canada Foundation for Innovation and the Marie Curie Action FP7-PEOPLE-IOF-2011 (Project: CHEMBC, No. 299755). N. Riemer and M. West acknowledge funding from the Department of Energy under Grant DOE DE-SC0011771.

References

Adachi, K. and Buseck, P. R.: Changes of ns-soot mixing states and shapes in an urban area during CalNex, J. Geophys. Res.-Atmos., 118, 3723–3730, 2013. 33559

ACPD
15, 33555–33582, 2015

Adachi, K., Freney, E. J., and Buseck, P. R.: Shapes of internally mixed hygroscopic aerosol particles after deliquescence, and their effect on light scattering, Geophys. Res. Lett., 38, L13804, doi:10.1029/2011GL047540, l13804, 2011. 33567

Adachi, K., Zaizen, Y., Kajino, M., and Igarashi, Y.: Mixing state of regionally transported soot particles and the coating effect on their size and shape at a mountain site in Japan, J. Geophys. Res.-Atmos., 119, 5386–5396, doi:10.1002/2013JD020880, 2014. 33559

Bond, T. C., Doherty, S. J., Fahey, D. W., Forster, P. M., Berntsen, T., DeAngelo, B. J., Flanner, M. G., Ghan, S., Kärcher, B., Koch, D., Kinne, S., Kondo, Y., Quinn, P. K., Sarofim, M. C., Schultz, M. G., Schulz, M., Venkataraman, C., Zhang, H., Zhang, S., Bellouin, N., Guttikunda, S. K., Hopke, P. K., Jacobson, M. Z., Kaiser, J. W., Klimont, Z., Lohmann, U., Schwarz, J. P., Shindell, D., Storelvmo, T., Warren, S. G., and Zender, C. S.: Bounding the role of black carbon in the climate system: a scientific assessment, J. Geophys. Res.-Atmos., 118, 5380–5552, 2013. 33557, 33558

Canagaratna, M. R., Jayne, J. T., Ghertner, D. A., Herndon, S., Shi, Q., Jimenez, J. L., Silva, P. J., Williams, P., Lanni, T., Drewnick, F., Demerjian, K. L., Kolb, C. E., and Worsnop, D. R.: Chase studies of particulate emissions from in-use New York City vehicles, Aerosol Sci. Tech., 38, 555–573, 2004. 33563

Cappa, C. D., Onasch, T. B., Massoli, P., Worsnop, D. R., Bates, T. S., Cross, E. S., Davidovits, P., Hakala, J., Hayden, K. L., Jobson, B. T., Kolesar, K. R., Lack, D. A., Lerner, B. M., Li, S. M., Mellon, D., Nuaaman, I., Olfert, J. S., Petaja, T., Quinn, P. K., Song, C., Subramanian, R., Williams, E. J., and Zaveri, R. A.: Radiative absorption enhancements due to the mixing state of atmospheric black carbon, Science, 337, 1078–1081, 2012. 33558, 33567

Chin, M., Kahn, R., Rind, D., Feingold, G., Schwartz, S., and DeCola, P.: Atmospheric Aerosol Properties and Climate Impacts, A Report by the U.S. Climate Change Science Program and the Subcommittee on Global Change Research, Tech. Rep. SAP 2.3, NASA, Washington, D.C., 2009. 33567

China, S., Salvadori, N., and Mazzoleni, C.: Effect of traffic and driving characteristics on morphology of atmospheric soot particles at freeway on-ramps, Environ. Sci. Technol., 48, 3128–3135, 2014. 33559

China, S., Scarnato, B., Owen, R., Zhang, B., Ampadu, M., Kumar, S., Dzepina, K., Dziobak, M., Fialho, P., Perlinger, J., Hueber, J., D. Helmig, Mazzoleni, L., and Mazzoleni, C.: Morphology and mixing state of aged soot particles at a remote marine free troposphere site: implications for optical properties, Geophys. Res. Lett., 42, 1243–1250, 2015. 33567

ACPD
15, 33555–33582, 2015

Ching, J., Riemer, N., and West, M.: Impacts of black carbon mixing state on black carbon nucleation scavenging: insights from a particle-resolved model, J. Geophys. Res.-Atmos., 117, D23209, doi:10.1029/2012JD018269, 2012. 33563
Chirico, R., DeCarlo, P. F., Heringa, M. F., Tritscher, T., Richter, R., Prévôt, A. S. H., Dommen, J., Weingartner, E., Wehrle, G., Gysel, M., Laborde, M., and Baltensperger, U.: Impact of aftertreatment devices on primary emissions and secondary organic aerosol formation potential from in-use diesel vehicles: results from smog chamber experiments, Atmos. Chem. Phys., 10, 11545–11563, doi:10.5194/acp-10-11545-2010, 2010. 33558
Chung, S. H. and Seinfeld, J. H.: Climate response of direct radiative forcing of anthropogenic black carbon, J. Geophys. Res.-Atmos., 110, D11102, doi:10.1029/2004JD005441, 2005. 33567
Corbin, J. C., Sierau, B., Gysel, M., Laborde, M., Keller, A., Kim, J., Petzold, A., Onasch, T. B., Lohmann, U., and Mensah, A. A.: Mass spectrometry of refractory black carbon particles from six sources: carbon-cluster and oxygenated ions, Atmos. Chem. Phys., 14, 2591–2603, doi:10.5194/acp-14-2591-2014, 2014. 33566
Cross, E. S., Onasch, T. B., Canagaratna, M., Jayne, J. T., Kimmel, J., Yu, X.-Y., Alexander, M. L., Worsnop, D. R., and Davidovits, P.: Single particle characterization using a light scattering module coupled to a time-of-flight aerosol mass spectrometer, Atmos. Chem. Phys., 9, 7769–7793, doi:10.5194/acp-9-7769-2009, 2009. 33564
Dallmann, T. R., Onasch, T. B., Kirchstetter, T. W., Worton, D. R., Fortner, E. C., Herndon, S. C., Wood, E. C., Franklin, J. P., Worsnop, D. R., Goldstein, A. H., and Harley, R. A.: Characterization of particulate matter emissions from on-road gasoline and diesel vehicles using a soot particle aerosol mass spectrometer, Atmos. Chem. Phys., 14, 7585–7599, doi:10.5194/acp-14-7585-2014, 2014. 33558
DeVille, R., Riemer, N., and West, M.: Weighted Flow Algorithms (WFA) for stochastic particle coagulation, J. Comput. Phys., 230, 8427–8451, 2011. 33562
Fast, J. D., Gustafson, W. I., Easter, R. C., Zaveri, R. A., Barnard, J. C., Chapman, E. G., Grell, G. A., and Peckham, S. E.: Evolution of ozone, particulates, and aerosol direct radiative forcing in the vicinity of Houston using a fully coupled meteorology-chemistry-aerosol model, J. Geophys. Res.-Atmos., 111, D21305, doi:10.1029/2005JD006721, 2006. 33567
Fierce, L., Riemer, N., and Bond, T. C.: When is cloud condensation nuclei activity sensitive to particle characteristics at emission?, J. Geophys. Res.-Atmos., 118, 13476–13488, doi:10.1002/2013JD020608, 2013. 33563

ACPD
15, 33555–33582, 2015

Freutel, F., Drewnick, F., Schneider, J., Klimach, T., and Borrmann, S.: Quantitative single-particle analysis with the Aerodyne aerosol mass spectrometer: development of a new classification algorithm and its application to field data, Atmos. Meas. Tech., 6, 3131–3145, doi:10.5194/amt-6-3131-2013, 2013. 33564

Healy, R. M., Sciare, J., Poulain, L., Kamili, K., Merkel, M., Müller, T., Wiedensohler, A., Eckhardt, S., Stohl, A., Sarda-Estève, R., McGillicuddy, E., O'Connor, I. P., Sodeau, J. R., and Wenger, J. C.: Sources and mixing state of size-resolved elemental carbon particles in a European megacity: Paris, Atmos. Chem. Phys., 12, 1681–1700, doi:10.5194/acp-12-1681-2012, 2012. 33558

Healy, R. M., Wang, J. M., Jeong, C.-H., Lee, A. K. Y., Willis, M. D., Jaroudi, E., Zimmerman, N., Hilker, N., Murphy, M., Eckhardt, S., Stohl, A., Abbatt, J. P. D., Wenger, J. C., and Evans, G. J.: Light-absorbing properties of ambient black carbon and brown carbon from fossil fuel and biomass burning sources, J. Geophys. Res.-Atmos., 120, 6619–6633, doi:10.1002/2015JD023382, 2015. 33562, 33567

Jacobson, M. Z.: A physically-based treatment of elemental carbon optics: implications for global direct forcing of aerosols, Geophys. Res. Lett., 27, 217–220, doi:10.1029/1999GL010968, 2000. 33559

Jacobson, M. Z.: Strong radiative heating due to the mixing state of black carbon in atmospheric aerosols, Nature, 409, 695–697, 2001. 33557

Jimenez, J. L., Jayne, J. T., Shi, Q., Kolb, C. E., Worsnop, D. R., Yourshaw, I., Seinfeld, J. H., Flagan, R., Zhang, X., Smith, K., Morris, J., and Davidovits, P.: Ambient aerosol sampling using the Aerodyne Aerosol Mass Spectrometer, J. Geophys. Res.-Atmos., 108, 8425, doi:10.1029/2001JD001213, 2003. 33561

Johnson, K. S., Zuberi, B., Molina, L. T., Molina, M. J., Iedema, M. J., Cowin, J. P., Gaspar, D. J., Wang, C., and Laskin, A.: Processing of soot in an urban environment: case study from the Mexico City Metropolitan Area, Atmos. Chem. Phys., 5, 3033–3043, doi:10.5194/acp-5-3033-2005, 2005. 33558

Kaiser, J. C., Riemer, N., and Knopf, D. A.: Detailed heterogeneous oxidation of soot surfaces in a particle-resolved aerosol model, Atmos. Chem. Phys., 11, 4505–4520, doi:10.5194/acp-11-4505-2011, 2011. 33563

Knox, A., Evans, G. J., Brook, J. R., Yao, X., Jeong, C. H., Godri, K. J., Sabaliauskas, K., and Slowik, J. G.: Mass absorption cross-section of ambient black carbon aerosol in relation to chemical age, Aerosol Sci. Tech., 43, 522–532, 2009. 33558

Kuwata, M., Kondo, Y., and Takegawa, N.: Critical condensed mass for activation of black carbon as cloud condensation nuclei in Tokyo, J. Geophys. Res.-Atmos., 114, D20202, doi:10.1029/2009JD012086, 2009. 33558

Laborde, M., Crippa, M., Tritscher, T., Jurányi, Z., Decarlo, P. F., Temime-Roussel, B., Marchand, N., Eckhardt, S., Stohl, A., Baltensperger, U., Prévôt, A. S. H., Weingartner, E., and Gysel, M.: Black carbon physical properties and mixing state in the European megacity Paris, Atmos. Chem. Phys., 13, 5831–5856, doi:10.5194/acp-13-5831-2013, 2013. 33558, 33559

Lack, D. A., Langridge, J. M., Bahreini, R., Cappa, C. D., Middlebrook, A. M., and Schwarz, J. P.: Brown carbon and internal mixing in biomass burning particles, P. Natl. Acad. Sci. USA, 109, 14802–14807, 2012. 33558

Lee, A. K. Y., Willis, M. D., Healy, R. M., Onasch, T. B., and Abbatt, J. P. D.: Mixing state of carbonaceous aerosol in an urban environment: single particle characterization using the soot particle aerosol mass spectrometer (SP-AMS), Atmos. Chem. Phys., 15, 1823–1841, doi:10.5194/acp-15-1823-2015, 2015. 33560, 33561, 33562, 33563, 33564, 33565

Liu, D., Allan, J., Whitehead, J., Young, D., Flynn, M., Coe, H., McFiggans, G., Fleming, Z. L., and Bandy, B.: Ambient black carbon particle hygroscopic properties controlled by mixing state and composition, Atmos. Chem. Phys., 13, 2015–2029, doi:10.5194/acp-13-2015-2013, 2013. 33558

Liu, D., Allan, J. D., Young, D. E., Coe, H., Beddows, D., Fleming, Z. L., Flynn, M. J., Gallagher, M. W., Harrison, R. M., Lee, J., Prevot, A. S. H., Taylor, J. W., Yin, J., Williams, P. I., and Zotter, P.: Size distribution, mixing state and source apportionment of black carbon aerosol in London during wintertime, Atmos. Chem. Phys., 14, 10061–10084, doi:10.5194/acp-14-10061-2014, 2014. 33559

Liu, S., Russell, L. M., Sueper, D. T., and Onasch, T. B.: Organic particle types by single-particle measurements using a time-of-flight aerosol mass spectrometer coupled with a light scattering module, Atmos. Meas. Tech., 6, 187–197, doi:10.5194/amt-6-187-2013, 2013. 33564

Liu, S., Aiken, A. C., Gorkowski, K., Dubey, M., Cappa, C. D., Williams, L. R., Herndon, S. C., Massoli, P., Fortner, E. C., Chhabra, P., Brooks, W., Onasch, T. B., Jayne, J. T., Worsnop, D., China, S., Sharma, N., Mazzoleni, C., Xu, L., Ng, N., Liu, D., Allan, J. D. Lee, J., Fleming, Z. L. Mohr, C., Zotter, P., Szidat, P., and Prevot, A. S. H.: Enhanced light absorption by mixed source black and brown carbon particles in UK winter, Nature Communications, 6, 8435, doi:10.1038/ncomms9435, 2015. 33558, 33567

ACPD
15, 33555–33582, 2015

Black carbon mixing state

M. D. Willis et al.

Title Page
Abstract | Introduction
Conclusions | References
Tables | Figures
◂◂ | ▸▸
◂ | ▸
Back | Close
Full Screen / Esc
Printer-friendly Version
Interactive Discussion

Massoli, P., Fortner, E. C., Canagaratna, M. R., Williams, L. R., Zhang, Q., Sun, Y., Schwab, J. J., Trimborn, A., Onasch, T. B., Demerjian, K. L., Kolb, C. E., Worsnop, D. R., and Jayne, J. T.: Pollution gradients and chemical characterization of particulate matter from vehicular traffic near major roadways: results from the 2009 Queens College Air Quality Study in NYC, Aerosol Sci. Tech., 46, 1201–1218, 2012. 33558, 33563

Matsui, H., Koike, M., Kondo, Y., Moteki, N., Fast, J. D., and Zaveri, R. A.: Development and validation of a black carbon mixing state resolved three-dimensional model: aging processes and radiative impact, J. Geophys. Res.-Atmos., 118, 2304–2326, doi:10.1029/2012JD018446, 2013. 33559, 33567

McComiskey, A., Schwartz, S., Schmid, B., Guan, H., Lewis, E., Ricchiazzi, P., and Ogren, J.: Direct aerosol forcing: calculation from observables and sensitivities to inputs, J. Geophys. Res., 113, D09202, doi:10.1029/2007JD009170, 2008. 33559, 33567

McMeeking, G. R., Good, N., Petters, M. D., McFiggans, G., and Coe, H.: Influences on the fraction of hydrophobic and hydrophilic black carbon in the atmosphere, Atmos. Chem. Phys., 11, 5099–5112, doi:10.5194/acp-11-5099-2011, 2011a. 33558

McMeeking, G. R., Morgan, W. T., Flynn, M., Highwood, E. J., Turnbull, K., Haywood, J., and Coe, H.: Black carbon aerosol mixing state, organic aerosols and aerosol optical properties over the United Kingdom, Atmos. Chem. Phys., 11, 9037–9052, doi:10.5194/acp-11-9037-2011, 2011b. 33558, 33559

Michelotti, M., Heath, M., and West, M.: Binning for efficient stochastic multiscale particle simulations, Multiscale Model Sim., 11, 1071–1096, 2013. 33562

Moffet, R. C. and Prather, K. A.: In-situ measurements of the mixing state and optical properties of soot with implications for radiative forcing estimates, P. Natl. Acad. Sci. USA, 106, 11872–11877, 2009. 33558

Mohr, C., Huffman, J. A., Cubison, M. J., Aiken, A. C., Docherty, K. S., Kimmel, J. R., Ulbrich, I. M., Hannigan, M., and Jimenez, J. L.: Characterization of primary organic aerosol emissions from meat cooking, trash burning, and motor vehicles with high-resolution aerosol mass spectrometry and comparison with ambient and chamber observations, Environ. Sci. Technol., 43, 2443–2449, 2009. 33563

Moteki, N., Kondo, Y., Miyazaki, Y., Takegawa, N., Komazaki, Y., Kurata, G., Shirai, T., Blake, D. R., Miyakawa, T., and Koike, M.: Evolution of mixing state of black carbon particles: aircraft measurements over the western Pacific in March 2004, Geophys. Res. Lett., 34, L11803, doi:10.1029/2006GL028943, 2007. 33558

Onasch, T. B., Trimborn, A., Fortner, E. C., Jayne, J. T., Kok, G. L., Williams, L. R., Davidovits, P., and Worsnop, D. R.: Soot particle aerosol mass spectrometer: development, validation, and initial application, Aerosol Sci. Tech., 46, 804–817, 2012. 33560, 33561

Oshima, N., Koike, M., Zhang, Y., and Kondo, Y.: Aging of black carbon in outflow from anthropogenic sources using a mixing state resolved model: 2. Aerosol optical properties and cloud condensation nuclei activities, J. Geophys. Res.-Atmos., 114, D18202, doi:10.1029/2008JD011681, d18202, 2009. 33559

Paatero, P. and Tapper, U.: Positive matrix factorization: a non-negative factor model with optimal utilization of error estimate of data values, Environmetrics, 5, 111–126, 1994. 33561

Ramanathan, V. and Carmichael, G.: Global and regional climate changes due to black carbon, Nat. Geosci., 1, 221–227, 2008. 33557

Riemer, N., West, M., Zaveri, R. A., and Easter, R. C.: Simulating the evolution of soot mixing state with a particle-resolved aerosol model, J. Geophys. Res.-Atmos., 114, D09202, doi:10.1029/2008JD011073, 2009. 33562, 33563, 33566

Riemer, N., West, M., Zaveri, R., and Easter, R.: Estimating soot aging time scales with a particle-resolved aerosol model, Aerosol Sci., 41, 143–158, 2010. 33563

Sabaliauskas, K., Jeong, C.-H., Yao, X., and Evans, G. J.: The application of wavelet decomposition to quantify the local and regional sources of ultrafine particles in cities, Atmos. Environ., 95, 249–257, doi:10.1016/j.atmosenv.2014.05.035, 2014. 33560

Sage, A. M., Weitkamp, E. A., Robinson, A. L., and Donahue, N. M.: Evolving mass spectra of the oxidized component of organic aerosol: results from aerosol mass spectrometer analyses of aged diesel emissions, Atmos. Chem. Phys., 8, 1139–1152, doi:10.5194/acp-8-1139-2008, 2008. 33564

Scarnato, B. V., Vahidinia, S., Richard, D. T., and Kirchstetter, T. W.: Effects of internal mixing and aggregate morphology on optical properties of black carbon using a discrete dipole approximation model, Atmos. Chem. Phys., 13, 5089–5101, doi:10.5194/acp-13-5089-2013, 2013. 33567

Schneider, J., Weimer, S., Drewnick, F., Borrmann, S., Helas, G., Gwaze, P., Schmid, O., Andreae, M. O., and Kirchner, U.: Mass spectrometric analysis and aerodynamic properties of various types of combustion-related aerosol particles, Int. J. Mass Spectrom., 258, 37–49, 2006. 33558

Seuper, D.: ToF-AMS analysis software, available at: http://cires.colorado.edu/jimenez-group/ToFAMSResources/ToFSoftware/index.html (last access: 24 September 2015), 2010. 33561

ACPD
15, 33555–33582, 2015

Shindell, D., Kuylenstierna, J. C. I., Vignati, E., van Dingenen, R., Amann, M., Klimont, Z., Anenberg, S. C., Muller, N., Janssens-Maenhout, G., Raes, F., Schwartz, J., Faluvegi, G., Pozzoli, L., Kupiainen, K., Hoglund-Isaksson, L., Emberson, L., Streets, D., Ramanathan, V., Hicks, K., Oanh, N. T. K., Milly, G., Williams, M., Demkine, V., and Fowler, D.: Simultaneously mitigating near-term climate change and improving human health and food security, Science, 335, 183–189, 2012. 33559

Shiraiwa, M., Kondo, Y., Moteki, N., Takegawa, N., Sahu, L. K., Takami, A., Hatakeyama, S., Yonemura, S., and Blake, D. R.: Radiative impact of mixing state of black carbon aerosol in Asian outflow, J. Geophys. Res.-Atmos., 113, D24210, doi:10.1029/2008JD010546, 2008. 33559

Tian, J., Riemer, N., West, M., Pfaffenberger, L., Schlager, H., and Petzold, A.: Modeling the evolution of aerosol particles in a ship plume using PartMC-MOSAIC, Atmos. Chem. Phys., 14, 5327–5347, doi:10.5194/acp-14-5327-2014, 2014. 33563

Toner, S. M., Sodeman, D. A., and Prather, K. A.: Single particle characterization of ultrafine and accumulation mode particles from heavy duty diesel vehicles using aerosol time-of-flight mass spectrometry, Environ. Sci. Technol., 40, 3912–3921, 2006. 33558

Tritscher, T., Juranyi, Z., Martin, M., Chirico, R., Gysel, M., Heringa, M. F., DeCarlo, P. F., Sierau, B., Prevot, A. S. H., Weingartner, E., and Baltensperger, U.: Changes of hygroscopicity and morphology during ageing of diesel soot, Environ. Res. Lett., 6, 034026, doi:10.1088/1748-9326/6/3/034026, 2011. 33558

Ulbrich, I. M., Canagaratna, M. R., Zhang, Q., Worsnop, D. R., and Jimenez, J. L.: Interpretation of organic components from Positive Matrix Factorization of aerosol mass spectrometric data, Atmos. Chem. Phys., 9, 2891–2918, doi:10.5194/acp-9-2891-2009, 2009. 33561, 33565

Wang, J. M., Jeong, C.-H., Zimmerman, N., Healy, R. M., Wang, D. K., Ke, F., and Evans, G. J.: Plume-based analysis of vehicle fleet air pollutant emissions and the contribution from high emitters, Atmos. Meas. Tech., 8, 3263–3275, doi:10.5194/amt-8-3263-2015, 2015. 33565

Willis, M. D., Lee, A. K. Y., Onasch, T. B., Fortner, E. C., Williams, L. R., Lambe, A. T., Worsnop, D. R., and Abbatt, J. P. D.: Collection efficiency of the soot-particle aerosol mass spectrometer (SP-AMS) for internally mixed particulate black carbon, Atmos. Meas. Tech., 7, 4507–4516, doi:10.5194/amt-7-4507-2014, 2014. 33561, 33562

ACPD

15, 33555–33582, 2015

Black carbon mixing state

M. D. Willis et al.

Zaveri, R. A. and Peters, L. K.: A new lumped structure photochemical mechanism for large-scale applications, J. Geophys. Res.-Atmos., 104, 30387–30415, doi:10.1029/1999JD900876, 1999. 33562
Zaveri, R. A., Easter, R. C., and Peters, L. K.: A computationally efficient multicomponent equilibrium solver for aerosols (MESA), J. Geophys. Res.-Atmos., 110, D24203, doi:10.1029/2004JD005618, 2005a. 33562
Zaveri, R. A., Easter, R. C., and Wexler, A. S.: A new method for multicomponent activity coefficients of electrolytes in aqueous atmospheric aerosols, J. Geophys. Res.-Atmos., 110, D02201, doi:10.1029/2004JD004681, 2005b. 33562
Zaveri, R. A., Easter, R. C., Fast, J. D., and L. K., P.: Model for Simulating Aerosol Interactions and Chemistry (MOSAIC), J. Geophys. Res., 113, 13204, doi:10.1029/2007JD008782, 2008. 33562, 33566
Zaveri, R., Barnard, J., Easter, R., Riemer, N., and West, M.: Particle-resolved simulation of aerosol size, composition, mixing state, and the associated optical and cloud condensation nuclei activation properties in an evolving urban plume, J. Geophys. Res., 115, D17210, doi:10.1029/2009JD013616, 2010. 33559, 33563, 33567
Zhang, G., Bi, X., Li, L., Chan, L. Y., Li, M., Wang, X., Sheng, G., Fu, J., and Zhou, Z.: Mixing state of individual submicron carbon-containing particles during spring and fall seasons in urban Guangzhou, China: a case study, Atmos. Chem. Phys., 13, 4723–4735, doi:10.5194/acp-13-4723-2013, 2013. 33558
Zhang, Q., Jimenez, J. L., Canagaratna, M. R., Ulbrich, I. M., Ng, N., Worsnop, D., and Sun, Y.: Understanding atmospheric organic aerosols via factor analysis of aerosol mass spectrometry: a review, Anal. Bioanal. Chem., 401, 3045–3067, doi:10.1007/s00216-011-5355-y, 2011. 33561, 33565
Zhang, R. Y., Khalizov, A. F., Pagels, J., Zhang, D., Xue, H. X., and McMurry, P. H.: Variability in morphology, hygroscopicity, and optical properties of soot aerosols during atmospheric processing, P. Natl. Acad. Sci. USA, 105, 10291–10296, 2008. 33558
Zhao, C., Liu, X., Qian, Y., Yoon, J., Hou, Z., Lin, G., McFarlane, S., Wang, H., Yang, B., Ma, P.-L., Yan, H., and Bao, J.: A sensitivity study of radiative fluxes at the top of atmosphere to cloud-microphysics and aerosol parameters in the community atmosphere model CAM5, Atmos. Chem. Phys., 13, 10969–10987, doi:10.5194/acp-13-10969-2013, 2013. 33567

ACPD
15, 33555–33582, 2015

Black carbon mixing state

M. D. Willis et al.

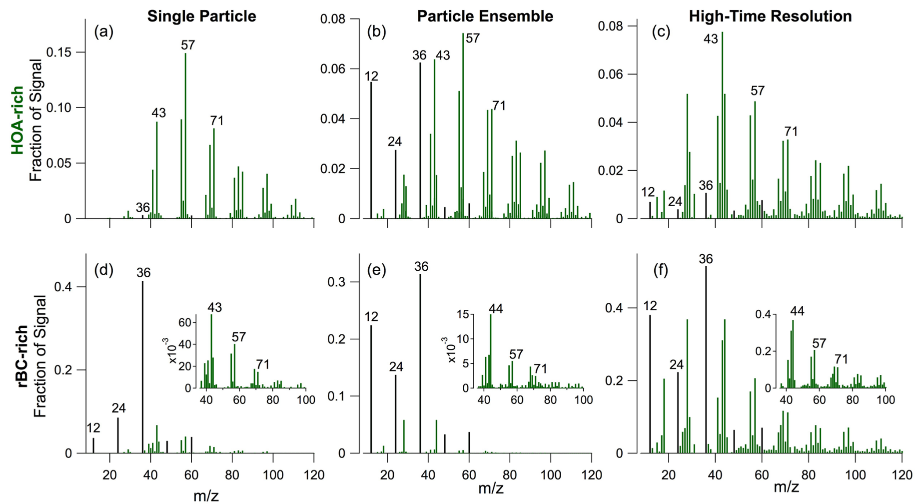

Figure 1. Left: unit mass resolution (UMR) spectra of HOA-rich **(a)** and rBC-rich **(d)** particle classes identified by *k*-means cluster analysis of single particle SP-AMS data acquired in the roadside environment. Middle: high-resolution mass spectra of HOA-rich **(b)** and rBC-rich **(e)** PMF factors from ensemble data. Right: examples of UMR spectra collected at high-time resolution during HOA-rich **(c)** and rBC-rich **(f)** plumes (corresponding time series are shown in Fig. 5). Insets in the lower panels illustrate the UMR spectrum of organic species (without CO_x^+ fragments) in the rBC-rich mass spectra. Black and colored sticks represent the fragments of rBC (C_x^+) and organic species($C_xH_y^+$,$C_xH_yO_w^+$), respectively.

ACPD
15, 33555–33582, 2015

Black carbon mixing state

M. D. Willis et al.

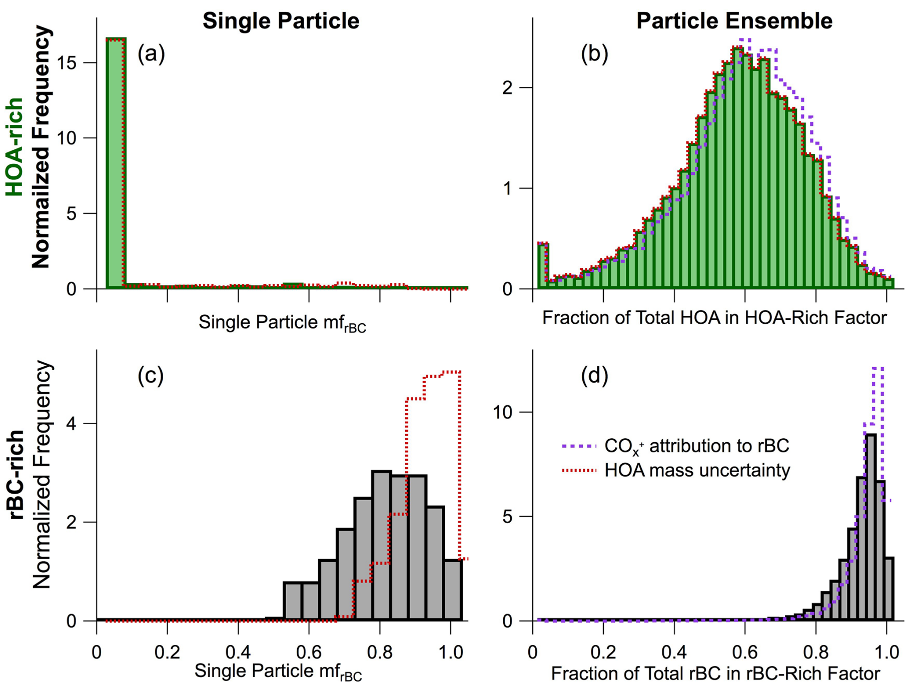

Figure 2. The distribution of mf_{rBC} (presented as a normalized histogram) in the HOA-rich and rBC-rich particle classes (**a** and **c**) measured in the roadside environment. Normalized histograms of mf_{Org} in the HOA-rich factor **(b)** and mf_{rBC} in the rBC-rich factor **(d)**, i.e., frequency distribution showing the fraction of total rBC (HOA) contributed by the rBC-rich (HOA-rch) factor. Bars represent mf_{rBC} calculated by rBC fragments (i.e. C_x^+), whereas purple dashed lines represent the mf_{rBC} calculated including both CO_x^+ and C_x^+ fragments, yielding similar results (see Supplement Sect. S1). Red dashed lines represent the impact of a 50 % decrease in HOA mass loading, to illustrate the impact of uncertainty in HOA quantification (see Supplement Sect. S1).

ACPD
15, 33555–33582, 2015

Black carbon mixing state

M. D. Willis et al.

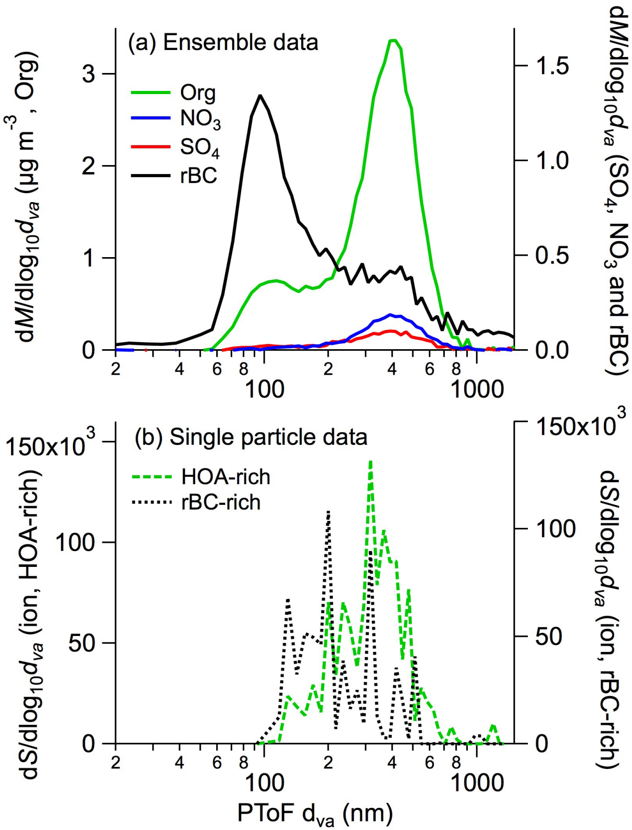

Figure 3. Particle size distributions from the roadside study. **(a)** Mass-based ensemble size distribution of refractory black carbon (rBC, black), organic species (Org, green), sulphate (SO_4, red) and nitrate (NO_3, blue). **(b)** Ion-signal based single particle size distributions for HOA-rich and rBC-rich particle classes. Analagous size distributions from the non-roadside study are shown in Fig. S3 in the Supplement.

ACPD
15, 33555–33582, 2015

Title Page
Abstract Introduction
Conclusions References
Tables Figures
◂ ▸
Back Close
Full Screen / Esc
Printer-friendly Version
Interactive Discussion

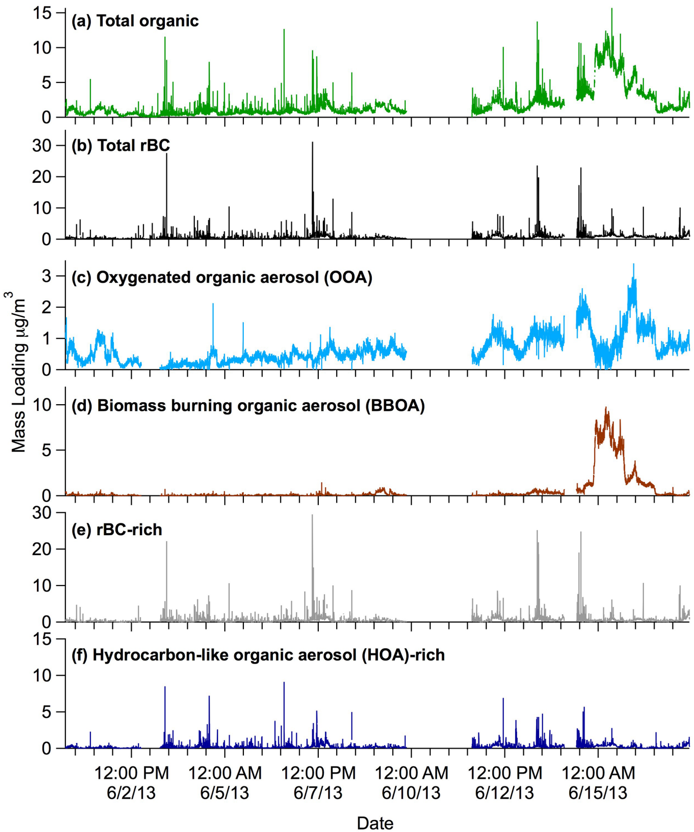

Figure 4. Time series of **(a)** ensemble organic aerosol and **(b)** refractory black carbon mass loadings during the roadside study. Positive matrix factorization (PMF) results for ensemble data **(c)** to **(f)**: **(c)** regionally sourced rBC mixed with oxygenated organic aerosol, **(d)** biomass-burning organic aerosol mixed with rBC, and traffic-related rBC in an rBC-rich and HOA-rich factor **(e, f)**. Mass spectra of all PMF factors are shown in Fig. S4 in the Supplement.

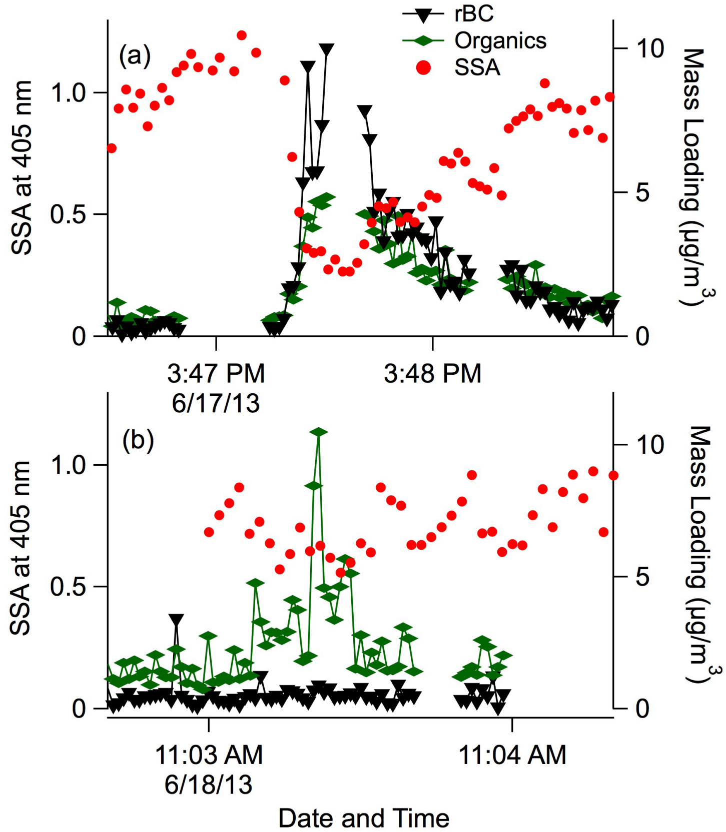

Figure 5. Examples of rBC-dominated **(a)** and organic-dominated **(b)** plumes observed using the SP-AMS with high-time resolution (1 Hz) sampling, with measurements of single scattering albedo (SSA) at 405 nm from a photoacoustic soot spectrometer (PASS-3). Gaps in SP-AMS data correspond to periods used for the subtraction of gas-phase contributions from particle signals. Mass spectra shown in Fig. 1c and f correspond to plumes **(b, a)**, respectively.

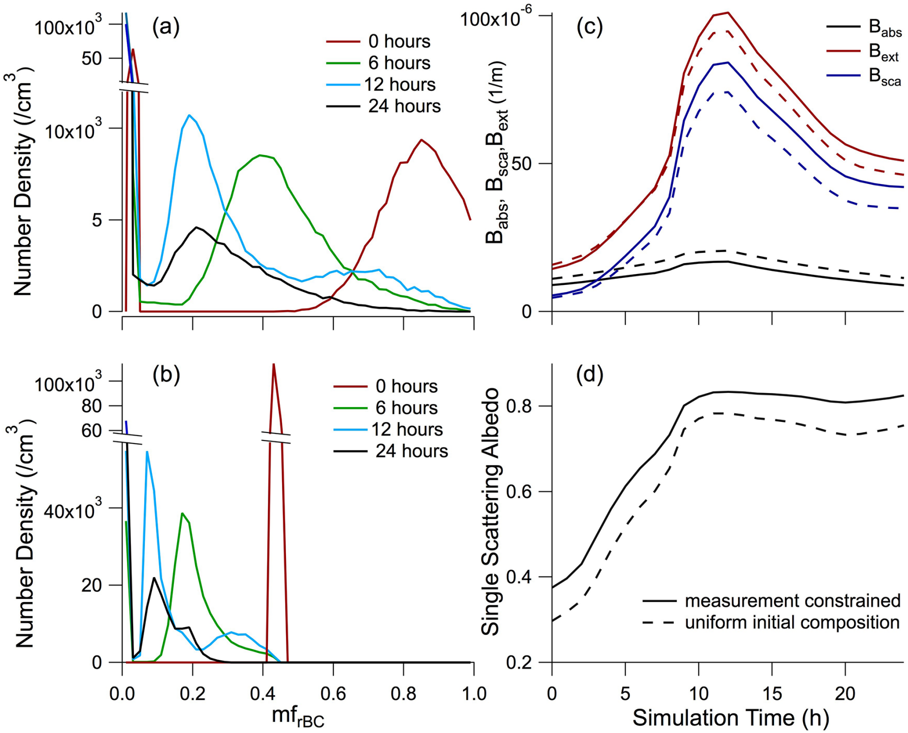

Figure 6. Evolution of dry mf_{rBC} for the measurement-constained **(a)** and uniform initial **(b)** mixing state cases. See Methods and Supplement Sect. S6 for a description of the model input parameters. Evolution of volume absorption (B_{abs}), scattering (B_{scat}) and extinction (B_{ext}) coefficients at 550 nm **(c)**, and single scattering albedo (SSA) at 550 nm over the 24 h simulation period **(d)** for measurement constrained (solid lines) and uniform initial mixing state (dashed lines) cases.